Faecalibacterium duncaniae A2-165 regulates the expression of butyrate synthesis, ferrous iron uptake, and stress-response genes based on acetate consumption

Sophie Verstraeten
Université Paris-Saclay, INRAE, Micalis Institute
Séverine Layec
Université Paris-Saclay, INRAE, Micalis Institute
Sandrine Auger
Université Paris-Saclay, INRAE, Micalis Institute
Catherine Juste
Université Paris-Saclay, INRAE, Micalis Institute
Céline Henry
Université Paris-Saclay, INRAE, Micalis Institute
Sawiya Charif
Université Paris-Saclay, INRAE, Micalis Institute
Yan Jaszczyszyn
Université Paris-Saclay, CEA, CNRS
Harry Sokol
Université Paris-Saclay, INRAE, Micalis Institute
Laurent Beney
Université Bourgogne Franche-Conté, UMR PAM
Philippe Langella
Université Paris-Saclay, INRAE, Micalis Institute
Muriel Thomas
Université Paris-Saclay, INRAE, Micalis Institute
Eugénie Huillet (eugenie.huillet@inrae.fr)
Université Paris-Saclay, INRAE, Micalis Institute

Research Article

Keywords: Faecalibacterium, Faecalibacterium duncaniae A2-165, acetate, butyrate, FeoB transporter, early stationary phase, RNA-Seq, Metaproteomics

Posted Date: March 8th, 2023

DOI: https://doi.org/10.21203/rs.3.rs-2481125/v2

Abstract

The promising next-generation probiotic *Faecalibacterium prausnitzii* is one of the most abundant acetate-consuming, butyrate-producing bacteria in the healthy human gut. Yet, little is known about how acetate availability affects this bacterium's gene expression strategies. Here, we show that, in the early stationary phase, *F. duncaniae* strain A2-165 (previously known as *F. prausnitzii*) can strongly regulate the expression of metabolic and stress-response genes based on acetate availability. Using RNA-seq, we compared gene expression patterns between two growth phases (late exponential vs. early stationary) and two acetate levels (low: 3 mM vs. high: 23 mM). Remarkably, transcription levels were high for the gene encoding the MAM protein, a pattern that was unaffected by acetate levels. At low-acetate levels, a general stress response was activated, and protein synthesis expression was down-regulated. At high-acetate levels, there was greater expression of genes related to butyrate synthesis and to the importation of B vitamins and iron. Specifically, expression was strongly activated in the case of the *feoAABC* operon, which encodes a FeoB ferrous iron transporter, but not in the case of the *feoAB*gene, which encodes a second FeoB transporter. RT-PCR revealed that excess ferrous iron repressed *feoB* gene expression. Finally, we detected FeoB peptides from strain A2-165 in a healthy human fecal metaproteome. In conclusion, we characterized two early stationary lifestyles for *F. duncaniae* A2-165 that relate to acetate consumption. Through multiomics and targeted approaches, this work highlights the crucial role that the

*feoAABC*operon might play in iron homeostasis in acetate-rich environments.

Introduction

Bacteria in the genus *Faecalibacterium* (phylum Firmicutes, class Clostridia*,* family Oscillospiraceae) are commensal, strictly anaerobic bacteria, that are ubiquitous and abundant in the gastrointestinal tracts of humans and animals [1, 2]. This genus is currently recognized as one of the most important commensals for human health [3, 4]. According to the latest phylogenetic analysis [5], the genus *Faecalibacterium* is composed of six species, of which *prausnitzii* is the best known for its effects on human health. The most extensively studied strain of *F. prausnitzii*, A2-165, has been recently reclassified and placed into a new species, *duncaniae* sp. nov. Interest in *Faecalibacterium* has increased over the last decade, mostly in response to the pioneering study of Sokol *et al.* reporting a depletion of *F. duncaniae* A2-165 in Crohn's disease patients [6]. Since this report, many studies have confirmed reduced abundances of *Faecalibacterium* in patients with inflammatory bowel disease and metabolic diseases [7, 8], which has led to consider members of this genus into candidates for the development of diagnostic, prognostic, preventive or therapeutic approaches [9].

In the healthy human colon, *Faecalibacterium* are among the main bacteria responsible for the consumption of acetate and the production of butyrate. Butyrate is the preferred energy source for colonocytes and has anti-inflammatory properties that are generally considered to be beneficial to intestinal health [10, 11]. Recently, we demonstrated that *dact3*, an host gene linked to the Wnt/JNK pathway, mediates these *F. prausnitzii* anti-inflammatory effects [12]. In addition, several peptides originating from a single 15-kDa protein (Microbial Anti-inflammatory Molecule, MAM) have been identified in the supernatant of *F. duncaniae* A2-165 cultures [13-15], and these have been shown to alleviate chemically induced colitis in mice [16, 17]. The key enzyme for butyrate production is butyryl-*CoA*:acetate *CoA*-transferase, which consumes extracellular acetate and intracellular acetyl-*CoA* from butyryl-*CoA* to produce butyrate and acetyl-*CoA* [1, 18-20]. In addition to generating butyrate, this process also promotes growth, thus explaining the growth-stimulating effects of culture supplementation with a high amount of acetate (33–50 mM) [1, 20, 21]. In co-culture models, acetate cross-feeding between *Faecalibacterium* and acetate-producing bacteria such as *Bifidobacteria adolescentis* [22] or *Blautia hydrogenotrophica* [20] has been observed to enhance butyrate formation. A positive correlation between acetate consumption and butyrate production was also established *in vivo* between *F. duncaniae* A2-165 and *Bacteroidetes thetaiotaomicron* [23].

In the human gut, acetate is the most abundant short-chain fatty acid largely generated by the bacterial fermentation of dietary fibers. Its concentration fluctuates depending on various parameters, including age, health status, diet, and microbiota composition [24, 25]. To cope with such changes*, Faecalibacteria* have presumably developed regulatory systems that sense and respond to acetate

levels. These adaptive strategies would necessarily involve a well-coordinated gene expression network that takes into account both the physiological state of the bacteria (latency, exponential, stationary phases) and the environmental conditions (availability of acetate and other nutrients, physicochemical signals such as oxygen tension, pH, temperature). Although several recent studies have investigated the transcriptome of *F. duncaniae* [20, 26, 27], none has examined the effects of acetate across growth phases. In light of its proposed vital role in intestinal health, this information is critical for understanding the metabolism of *Faecalibacterium* and how this might affect human health.

Here, we investigated the effect of acetate on temporal changes in the transcriptome of *F. duncaniae* A2-165 cultures using RNA sequencing. Next, we characterized the regulation of two *feoB* genes -which encode well-known ferrous iron transporter- in response to the availability of acetate and ferrous sulfate. Finally, using an novel integrated approach, we searched for and identified FeoB peptides specific to the A2-165 strain in the healthy human fecal metaproteome. The general workflow of our study is presented in Figure S1 (Additional file 1).

Results

Experimental design for acetate-dependent transcriptome analysis

Acetate consumption is the main driver of butyrate production by genus *Faecalibacterium*, as shown in Figure 1A. To gain insight into the effect of acetate on the transcriptome of *F. duncaniae* A2-165, two sets of cultures were established in media that contained low (3 mM) or high (23 mM) concentrations of acetate. The resulting growth kinetics are shown in Figure 1B. In both acetate conditions, there was no difference in growth kinetics over the first 7 hours, and the stationary growth phase was reached after 9 hours of culture in both treatments. In the early stationary phase, the biomass in high-acetate conditions (Sa) was about 1.5-fold higher than in low-acetate conditions (S) (2.30 ± 0.13 OD_{600} *vs.* 1.50 ± 0.18 OD_{600}, N=4, $p < 0.05$). Moreover, the growth rate was 1.25-fold higher in high-acetate conditions (Fig. 1C), suggesting that the general metabolism of *F. duncaniae* A2-165 was highly active in these cultures. Indeed, the generation time was reduced by about 25 minutes in this group compared to that of low-acetate cultures (1.67 h *vs.* 2.08 h). In high- and low-acetate conditions, we quantified butyrate production and acetate consumption in both the late exponential growth phase (Ea and E, respectively) and the early stationary growth phase (Sa and S, respectively) (Fig. 1D). As expected, in both acetate conditions, butyrate production was significantly higher in the early stationary phase than in the late exponential phase. Moreover, in the late exponential phase (7 hours of growth) there was no difference between acetate conditions in either butyrate production or acetate consumption. In contrast, in the early stationary phase (10 hours of growth), butyrate production and acetate consumption were significantly different between acetate conditions (butyrate: 11.94 mM ± 0.89 for Sa, 6.37 mM ±1.07 for S, $p < 0.01$). Moreover, after 10 hours of growth, almost all acetate had been consumed in the low-acetate cultures (-2.16 mM ± 0.38), whereas only one-third of the acetate had been consumed in the high-acetate cultures

(-7.66 mM ± 0.58). The acetate limitation experienced in the low-acetate conditions strongly affected the growth of *F. duncaniae* A2-165 (Fig. 1BC). We thus investigated the acetate-growth effect at the transcriptional level in both acetate-limited and acetate-saturated conditions using RNA-Seq. For this, gene expression profiles were analyzed at both E/Ea and S/Sa time points (Fig. 1B).

Overview of transcriptomes in low- and high-acetate conditions

The RNA-Seq datasets contained a total of 2,882 genes out of the 3,013 predicted in the RefSeq database (i.e., over 95%). Of these, 1,161 genes were found to be differentially expressed (DE) ($\log_2$ fold change (FC) $\geq |2|$ and FDR-adjusted p-value ≤ 0.01) between conditions (Table S1 in Additional file 2). All DE genes are presented in Additional file 2 (Tables S2–S5). Eight of these genes were differentially expressed in early exponential cultures, compared to 542 in the late stationary phase (340 and 202 transcripts up- and down-regulated, respectively, Fig. 2A), which is consistent with the different patterns of growth kinetics. This result clearly demonstrates that, under our experimental conditions, acetate concentration (3 *vs.* 23 mM) had little impact on transcriptomic profiles in *F. duncaniae* A2-165 for the first 7 hours of growth (i.e., up to the late exponential growth phase), but had a significant impact when the cultures entered the stationary phase of growth. This prompted us to perform a detailed analysis of the adaptive changes that occur in the transcriptome in response to acetate availability between 7 and 10 hours of growth. As shown in Figure 2B, there was a large difference in the adaptive response between high-acetate (Sa/Ea, 118 DE genes) and low-acetate (S/E, 492 DE genes) conditions in this three-hour period. Specifically, we found that, under high-acetate conditions, only 67 and 51 genes were up- and downregulated, respectively, whereas under low-acetate conditions, 216 and 276 genes were up- and downregulated, respectively. When comparing the DE transcript lists in low- and high-acetate conditions (Sa/Ea compared to S/E, Fig. 2C), it clearly appeared that the acetate-limiting condition triggered a larger and more-specific adaptive transcriptional response at the onset of the stationary growth phase compared to the acetate-saturated conditions.

Using the COG and PATRIC databases, we classified DE genes into 12 functional categories (Table S6, Additional file 2). As shown in Figure 3A, for all transcriptomes (high-acetate, low-acetate, and early stationary), the largest category (27.2% to 58.8% of genes) was the superclass “Poorly characterized protein-genes”, which included the categories “Hypothetical proteins” and “General function prediction”. It is likely that these unknown DE genes contribute to the adaptive responses of *F. duncaniae* A2-165 as cells enter the stationary phase. In addition, clear differences between low- and high-acetate transcriptomes were observed with respect to the categories “Protein synthesis”, “Energy metabolism”, “Import system”, “Defense system”, “Stress response”, and “Transcription and Post-transcriptional regulation” (Fig. 3A, Table S6). Interestingly, in acetate-limiting conditions (S *vs.* E), the highest

proportions of up- and downregulated genes were related to “Stress response” (9.3%, i.e., 20 DE genes) and “Protein synthesis” (27.9%, i.e., 77 DE genes) respectively, whereas in acetate-saturated conditions (Sa *vs.* Ea), the highest proportions of affected genes were related to “Import system” (13.4%, i.e., 9 upregulated genes, and 23.5%, i.e., 12 downregulated genes).

Overall, our transcriptome analysis strongly suggests that *F. duncaniae* A2-165 is able to tightly regulate the expression of metabolic and stress-response genes according to acetate levels. Remarkably, in all comparative transcriptional analyses, the CG447_03795 gene encoding the MAM protein did not appear among the DE genes; the transcription of this gene was quite high and unchanged between acetate conditions as well as between the growth phases examined here (Fig. S2 in Additional file 3). To further characterize the acetate responses we observed, we investigated in more detail these functional categories: “Protein synthesis”, “Stress response”, “Transcription and Post-transcriptional regulation” and “Import system” (Fig. 3B).

A general stress response under acetate-limiting conditions

As depicted in Figure 3B, we clearly observed significant differences in the transcriptional responses of *F. duncaniae* A2-165 under acetate-limiting condition compared with acetate-saturated condition. Interestingly, in low-acetate condition, we found a high number of downregulated transcripts in the “Protein synthesis” category (77 DE genes, $\log_2$FC range: 2–5, Table S4) that were not detected in high-acetate condition. These were mainly transcripts involved in translation machinery, such as translation initiation/elongation factors and aminoacyl-tRNA synthetases/transferases, but also included genes involved in ribosome biogenesis and/or stability. These findings likely indicated a major slowdown of translational processes under low-acetate growth conditions as *F. duncaniae* cells entered the stationary phase.

We also noted a drastic shift in the “Stress response” category (20 DE genes, Table S4) which again was not observed in high-acetate condition. Seven of these genes ($\log_2$FC range: 2.2–2.9) encoded chaperone proteins involved in protein remodeling, in the repair of proteins following stress damage, or even in the ubiquitin machinery and proteasome. The remaining 13 ($\log_2$FC range: 2.1–6.2) genes were associated with type II toxin/antitoxin (TA) systems [28]. More specifically, we observed the upregulation of four putative operons for RelE TA systems, one putative operon for a TA module in the Doc family, two genes encoding antitoxin proteins, and one gene encoding a toxin protein. Of these, the DinJ/YafQ system (CG447_14090/14095) was the most activated TA system ($\log_2$FC: 6.1–6.2). Overall, our data suggest that cells of *F. duncaniae* A2-165 in low-acetate condition experienced severe general stress upon entry to the early stationary growth phase.

Bacteria employ different transcriptional regulators and sigma transcription factors to respond to changing environments. In the low-acetate transcriptome examined here, we found a higher number of upregulated genes encoding transcriptional regulators and sigma transcription factors (18 DE genes, log_2FC range: 2.1–5.5, Table S4) compared to high-acetate condition (4 DE genes, log_2FC range: 3.0–5.0, Table S5). Moreover, in all bacteria studied thus far, the global regulator that mediates the general stress response is a specialized sigma factor [29]. In the low-acetate transcriptome, we specifically found five upregulated genes encoding sigma factors (CG447_02225/05485/06440/06875/08160, Table S4), while in high-acetate conditions there was only one, which was also upregulated in low-acetate conditions (CG447_02215, Tables S4-S5). It is thus possible that these five sigma factors could be involved in the general stress response described above when cells enter the stationary phase.

Deciphering import systems under high- and low-acetate conditions

Transcription of transporter genes is usually regulated in response to substrate availability [30]. As shown in Figure 3B, we clearly observed two distinct import system transcriptomes of *F. duncaniae* A2-165, under acetate-limiting and saturated conditions. These findings likely indicated two major adaptation responses to substrate availability, according to acetate conditions. A large number of genes belonging to the “Import system” category were found to be downregulated under low-acetate conditions (46 DE genes, Table S4); this number was four-fold higher than under high-acetate conditions. These were mainly transporter genes in the ABC superfamily (25 DE genes), in the sodium-dependent transporter family (5 DE genes), in the ECF subfamily (3 DE genes) and in the FeoB family (3 DE genes) (Table S4). Within the ECF group, we noticed a reduction in gene expression related to B vitamins uptake (*bioY* gene CG447_11745, involved in biotin import, log_2 FC -4.14, *ribU* gene, CG447_14300, log_2 FC -3.92, involved in riboflavine import) (Fig.3B). Within the FeoB group, we noticed a considerable reduction in gene expression related to ferrous iron uptake (*feoAABC* putative operon, CG447_12740-55, log_2 FC range: -4.9–5.9, Fig.3B), and ferric iron uptake (*fhu* putative operon, CG447_03300-10, log_2FC range: -6.1–8.0). This suggested that the expression of major systems of iron transport was severely impaired in low-acetate conditions. Conversely, we found that expression of the *feoAABC* operon was upregulated under high-acetate condition (log_2FC: 1.5–2.1, Table S5, Fig.3B). This was particularly marked in early stationary transcriptome, in which we observed an even higher fold-change in expression (log_2FC: 4.5–5.9, Table S3, Fig.3B). Many studies have explored the role of the FeoB transporters in ferrous iron uptake in iron-poor environments [31, 32]. Our result suggests that in the early stationary phase in an acetate-saturated environment, ferrous iron is no longer abundant, and activation of the *feoAABC* system may allow *F. duncaniae* A2-165 cells to maintain iron homeostasis in these conditions.

Negative regulation of feoB, but not feoAB in the presence of ferrous sulfate in high-acetate conditions

In order to confirm our hypothesis of limited iron availability in the high-acetate culture conditions, we analyzed *feoB* expression in the presence of excess ferrous sulfate (Fig. 4). Figure 4A illustrates ferrous iron uptake and iron homeostasis in *F. duncaniae*. As a control, we also analyzed gene expression in low-acetate conditions, as well as the expression of *feoAB* (CG447_08795, $\log_2$FC: -4.3, Table S5, Fig. 3B) and *butCoA*, which encodes the terminal enzyme required for butyrate production (Fig. 4A). A new set of *F. duncaniae* A2-165 cultures was prepared with high or low levels of acetate and with or without ferrous sulfate, and sampling was performed as previously described (i.e., in the late exponential phase, indicated by E, and the early stationary phase, indicated by S, Fig. 4B). Figure 4B presents the results regarding the expression ratios of *feoB*, *feoAB*, and *butCoA* obtained under the different conditions. These clearly demonstrated that the *feoB* expression was strongly activated only in high-acetate condition. Moreover, its regulation was dependent on the availability of an iron source in the medium, with strong activation and repression in the absence and presence of ferrous sulfate, respectively. For the *feoAB* gene, the expression ratios were similar in the absence or presence of an iron source in both acetate growth conditions, indicating that the regulation of *feoAB* is independent of iron availability in our growth condition. For the *butCoA* gene, we observed a positive growth phase effect in both acetate and iron conditions with stronger activation in the high-acetate conditions (Fig. 4B). Overall, these results demonstrate that regulation of the expression of *feoAABC* and *feoAB* differs significantly and suggest that the FeoB and FeoAB systems of *F. duncaniae* A2-165 play nonredundant roles in ferrous iron acquisition.

FeoB peptides from F. duncaniae A2-165 detected in healthy human fecal samples

As our culture data suggested that *feoB* gene expression was tightly regulated, we were interested in studying its expression *in vivo*, in the human gut microbiome. For this, we analyzed a metaproteomic dataset obtained from eight healthy individuals, which included 123 425 peptides from the envelope fraction of the gut microbiota (Fig. 5) [33]. The metaproteomic data are presented in Additional file 4. Among these peptides, 236 matched with 10 of the 42 transporter genes that we had found to be upregulated in high-acetate conditions (Table S7 in additional file 2). Remarkably, the second highest degree of protein coverage (43.6%, 51 peptides) was found for the FeoB transporter. Of those 51 peptides, 9 were specific to a single protein in the metaproteomic dataset (‘a5.b59.a1’, sheet ‘CG447_12750 FeoB’ in Additional file 4), which was identified as FeoB of the A2-165 strain (K04759 in the KEGG orthology database). This demonstrated that the FeoB protein from A2-165 is expressed (i.e., transcribed and translated) in the human gut under healthy conditions. Furthermore, the fact that it was detected in four

of the subjects at different levels, but not in the remaining four, suggests that *feoB* is also tightly regulated *in vivo* in the human gut.

Discussion

Two early stationary lifestyles of F. duncaniae A2-165

The transition between nutrient-rich and -poor environments is a natural occurrence for all bacteria. Here, we investigated the adjustments in the bacterial transcriptome when cells of *F. duncaniae* A2-165 entered the stationary growth phase (i.e., nutrient-limited environment) in low- and high-acetate conditions. A characteristic of this transition is the induction of stress proteins adapted for general stress condition. The general stress response has been very well characterized in model bacteria such as *Escherichia coli* and *Bacillus subtilis* [34], but this protective adaptive response is not known in *Faecalibacterium*. Notably, a general stress response was observed only in low-acetate conditions; concomitantly with the general stress response, a negative regulation of protein synthesis genes and a positive regulation of genes encoding type II toxin/antitoxin modules were also observed. As the majority of type II toxins inhibit translation [28], we can hypothesize that the former observation may be the consequence of the latter. Sigma B is the sigma factor involved in the control of the general stress reponse [34] in many bacteria including model bacteria and several anaerobic bacteria such as *Clostridioides difficile* [35]. Remarkably, the gene encoding Sigma B is not present in A2-165 genome. Our functional analysis led to a list of genes encoding Sigma factors, that could be involved in the control of this protective response in low-acetate conditions. To our knowledge, this study represents the first description of the general stress response, in the early stationary phase, in acetate-limiting conditions in *Faecalibacterium*.

Comparative analysis of the high- and low-acetate transcriptomes showed two different metabolic responses regarding the number of genes and their functions. Given that acetate is a major growth factor, this seems consistent. Because of the lack of relevant data from the literature with which to compare our results, we chose to focus on the strongest and clearest effects, i.e., high fold-changes in expression. In the future, it will be necessary to study i) the functions carried by the weaker adjustments in the transcriptome (i.e. lower fold change); and ii) this adaptive response with other semi-synthetic culture media.

FeoB transporter, Iron homeostasis and butyrate production

In many environments, including the human gut, iron is a limiting nutrient for growth, and high-affinity uptake systems play a central role in ferrous iron homeostasis [36]. Altogether, our expression data strongly suggest that the *feoAABC* operon encodes a high-affinity ferrous iron transporter that may play a major role in ferrous iron homeostasis in iron-limited conditions. Maintenance of ferrous iron homeostasis is crucial for the production of butyrate [37] because this process requires two iron-binding ferredoxins as illustrated in Figure 4A. Here, we demonstrated that *butCoA* expression was strongly upregulated

regardless the supplementation of cultures with ferrous sulfate. This result suggests that, in the early stationary growth phase in high-acetate conditions, mechanisms of ferrous iron homeostasis were well established in *F. duncaniae* A2-165.

Interestingly, together with upregulation of *feoAABC*, we also detected upregulation of a flavodoxin-encoding gene (Table S5 in additional file 2). This is consistent with previous studies reporting that iron-free flavodoxin replaces iron-sulfur ferredoxin under iron-limited conditions [36, 38]. Because flavodoxin and ferredoxin both mediate electron transfer in redox processes, the use of flavodoxin could free up iron for utilization by other iron-dependent enzymes. In other word, flavodoxins are key players in maintenance of ferrous iron homeostasis in iron-limited environment [36, 38]. For example, in *C. difficile*, the production of flavodoxin is tied to iron homeostasis in iron-limited conditions [39]. In addition, the switch to flavodoxin as electron transfer protein may have significant effects on the activity of numerous enzymes that use flavodoxin as a redox partner. For example, in *B. subtilis*, flavodoxin is the redox partner for the acyl lipid desaturase involved in fatty-acid desaturation [40]. To date, similar data are not available for *Faecalibacterium*, but the impact of flavodoxins on the activity of certain metabolic pathways, including butyrate pathway, as well as the link with iron availability, merits further investigation.

We believe that investigation of the complex protective and metabolic network that help *F. duncaniae* to adapt to nutrient-limited conditions,including iron and acetate, may improve our understanding of how this commensal bacterium is able to colonize and thrive as a dominant species in the human gut. In the future, detailed characterizations of the regulatory responses of *Faecalibacterium* with respect to acetate, iron and other available nutrients will help us to identify the conditions necessary for its proliferation in the gut and provides additional clues on the lifestyle requirements for several beneficial *Firmicutes*.

Conclusion

Commensal butyrate-producing bacteria in phylum Firmicutes are abundant in the human gut and are crucial for health. Using RNA-Seq, we characterized two early stationary lifestyles of *F. duncaniae* A2-165 related to acetate consumption and butyrate production. Moreover, by combining analyses of growth kinetics, SCFAs, RNA-Seq data, fecal metaproteomes, and gene expression, this work highlights the crucial role of the FeoB transporter in ferrous iron uptake, iron homeostasis, and butyrate production.

Methods

Strain used for experimental culture

This study used a stock of *Faecalibacterium duncaniae* A2-165 (DSM No. 17677, DSMZ collection, Braunschweig, Germany) originally isolated from human fecal stool by S. H. Duncan (University of Aberdeen, United Kingdom) [1] and maintained by V. Robert, MICALIS Institute, INRAE, France.

Cultivation experiments of F. duncaniae

F. duncaniae A2-165 was grown under anaerobic conditions (anaerobic chamber: N_2 = 90%, CO_2 = 5%, and H_2 = 5%) at 37°C in BHIS medium (also named LYBHI in our previous studies), which is brain heart infusion broth (BHI, 37 g/L, Difco) supplemented with yeast extract (5 g/L, Difco), cellobiose (1 mg/mL, Sigma), maltose (1 mg/mL, Sigma), and cysteine (0.5 mg/mL, Sigma) [16]. The strain was thawed and grown from a 10% inoculation in 10 mL BHIS for 24 hours at 37°C, followed by a 1% inoculation in 10 mL BHIS for overnight growth (16–18 hours). The experimental cultures were then created using 2% inoculation in 50 mL BHIS medium with (BHISAc) or without the addition of sodium-acetate solution (20 mM, Sigma, [1, 37]) at the time of inoculation. Growth kinetics were monitored by measuring the OD_{600} nm every hour.

Addition of ferrous sulfate to F. duncaniae culture

A fresh solution of ferrous sulfate ($FeSO_4$-$7H_20$, Sigma) was prepared with deionized water and filter-sterilized. The experimental cultures were created using 2% inoculations in 50 mL BHIS or BHISAc media. Ferrous sulfate (50 µM, Sigma) was added 3 hours after inoculation.

Short-chain fatty acid (SCFA) production and consumption

Gas chromatography (7890B, Agilent Technologies) was used to identify the short-chain fatty acids present in culture supernatants. The SCFAs of interest in this study were acetate and butyrate. An internal standard of 2-ethylbutyrate was used to normalize the data in each run. Measurements of SCFA concentrations in the bacterial samples were normalized using the basal SCFA levels of BHISAc and BHIS media from the same experiment.

Collection of RNA samples

For both growth conditions, cells and culture supernatant were sampled in the late exponential growth phase (7 hours after inoculation) and early stationary growth phase (10 hours after inoculation) for RNA extraction (cells) and SCFA analysis (supernatant). At the times of sampling, dilutions were created of all cultures and plated on BHIS agar for quantification of colony-forming units (CFUs).

RNA extraction

The single-step RNA isolation method was used, with TRIzol reagent and the FastPrep-24™ 5G instrument. For RNA-Seq and RT-PCR analyses, 2 ml of each culture was harvested and centrifuged (30 s, 13000 rpm) in the Freter chamber, and cell pellets were snap-frozen in liquid nitrogen. One ml of TRIzol reagent (phenol-based RNA extraction buffer, Ambion, ThermoFisher Scientific) and 0.4 g of glass beads (0.1 mm, Bühler, ThermoFisher Scientific) were added to the defrosted pellet, and cell lysis was performed with a FastPrep-24™ 5G instrument (MP Biomedicals) (speed 6, 40 s). RNA precipitation, washing, and solubilization was carried out following the TRIzol protocol. Residual DNA from the RNA preparations was enzymatically removed using TURBO DNA-free (Ambion, United Kingdom). RNA quality was

assessed with the Agilent 6000 Nano kit using an Agilent 2100 bioanalyzer (Stratagene, Agilent Technologies, France); RIN values were in the 7.7 to 8.5 range. Total RNA was purified from three biological replicates for RNA-Seq experiments and for RT-qPCR analysis. Extracted RNA samples were stored in RNAase/DNAse-free water (Ambion, United Kingdom) at -80°C.

Library construction and Illumina sequencing

Total RNA quality was assessed using an Agilent Bioanalyzer 2100 and the RNA 6000 Pico kit (Agilent Technologies). Directional RNA-Seq libraries were constructed using the TruSeq Stranded Total RNA library prep kit, with bacterial Ribo-Zero reagents (Illumina), following the manufacturer's instructions; 500 ng of total RNA were used (I2BC HTS platform, CNRS, Gif-sur-Yvettes, France). After the Ribo-Zero step, the samples were checked on the Agilent Bioanalyzer to verify rRNA depletion. The quality of the libraries was assessed on an Agilent Bioanalyzer 2100, using an Agilent High Sensitivity DNA Kit. Libraries were pooled in equimolar proportions and sequenced in a paired-end 2x75-pb run on an Illumina NextSeq500 instrument (I2BC HTS platform, CNRS, Gif-sur-Yvettes, France). Demultiplexing was performed with bcl2fastq2 v2.18.12. Adapters were trimmed with Cutadapt v1.15, and only reads longer than 10 pb were kept for further analysis.

Mapping and identification of differentially expressed genes

Reads were mapped on the genome of *F. duncaniae* strain A2-165 (GenBank: CP022479.1) with BWA 0.6.2-r126, and were counted using the subread feature of Counts v1.5.2. Analyses of differential expression were performed in R using DESeq2 (I2BC HTS platform, CNRS, Gif-sur-Yvettes, France). In total, 2,900 genes—including 2,819 protein-coding sequences, 63 tRNA genes, and 18 rRNA genes, were mapped. Only the first two groups were analyzed in this study, so that a total of 2,882 genes were considered. These were further filtered to retain only ORFs that showed a four-fold change in expression (absolute value Log_2FC >=2) (up/down) between treatment conditions. RNA-Seq datasets can be found on the database Omics Dataverse under the DOI accession number BDNCT2 (https://doi.org/10.15454/BDNCT2).

RT-PCR analysis

We generated cDNA from 1 µg of total RNA using the High Capacity cDNA Reverse Transcription kit (Fisher Scientific, France) and random hexamers. The quality of cDNA was checked with an Agilent 6000 Pico kit and an Agilent 2100 Bioanalyzer (Stratagene, Agilent Technologies, France). We carried out qPCR in duplicate, in a reaction volume of 20 µl containing 500 pg of cDNA, 15 µl of SYBR® Green PCR Master Mix (Applied Biosystems, Courtaboeuf, France), and 300 nM of each gene-specific primer. The primers were designed with Primer Express® (version 3.0). We generated standard curves for each set of primers,

using serial dilutions (four dilutions) of cDNA obtained from a mix of total RNA collected in BHISAc and BHIS. Amplification was carried out with an ABI® PRISM 7900 thermal cycler (Applied Biosystems), with the following thermal profile: 2 min at 50°C, 10 min at 95°C, and 40 cycles of 15 s at 95°C and 60 s at 60°C. The specificity of each PCR amplicon was checked by melting curve analysis. Here, the *feoB* (CG447_12750, F5'-tgatcttcaacctgctgtgc, R5'-gccacgatggtgaagaagtt), *feoAB* (CG447_08795, F5'-ataccgaagtcaccgacctg R5'- ctccatcagctgcatcgtta) and *butCoA* (CG447_01820, F5'-actttgttctgggcgcatac, R5' -ggtcagtcccttcaggttca) primers used in this study. The *efp* gene (CG447_05125), encoding the translation elongation factor P, was used for normalization with the primers *efpF* (5-gttgagttccagcacgtgaa-3) and *efpR* (5-aaagcctgagggaactttgc-3). The relative change in gene expression was recorded as the ratio of normalized target concentrations and was calculated with the comparative ΔΔCt - [41]. The mean values for three independent experiments are presented.

Protein sequence annotations, functional classification

The manually curated and validated genome reconstruction iFpraus_v1.0, which contains 602 genes of the A2-165 genome [37], was used for annotation correction. Protein annotation data from the PATRIC database [42] (PATRIC genome ID 853.173) were used for functional classification. As the functional subsystem coverage in PATRIC was low (29%), we manually generated COG-based functional classifications using the COG system (https://www.ncbi.nlm.nih.gov/research/COG).

We created a simplified classification scheme with 12 categories; the largest metabolism classes (protein synthesis, energy, and import system) were retained while smaller metabolism classes (cell wall metabolism, lipid metabolism, amino acid metabolism, amino sugar metabolism, nucleotide metabolism, vitamin & cofactor metabolism, bacterial cell division processes) were merged into an “Other metabolism” category. The “Import system” and “Export system” classes encompassed all membrane transport systems involved in the uptake/export processes of nutrients, micronutrients, ions, and unknown compounds. Subclasses were defined for import systems, transcriptional regulation, energy metabolism, defense mechanisms, and stress response. The TC-BLAST tool (TCD database https://www.tcdb.org/) was used for the determination of the number of TMS (putative TransMembrane Segment) and for the import system family assignment. To characterize gene similarity, homology, and gene context, NCBI BLAST was used, in particular for analysis of *feo* genes.

Statistical analysis

Normally distributed data are presented as mean ± standard deviation (SD), skewed data as median with interquartile range (IQR), and categorical data as frequencies with proportions. T-tests for independent samples and one-way analysis of variance (ANOVA) (or Kruskall-Wallis when not normally distributed) were performed for continuous variables. Data were represented and analyzed with GraphPad Prism 8.

References

1. Duncan SH, Hold GL, Harmsen HJM, Stewart CS, Flint HJ. Growth requirements and fermentation products of Fusobacterium prausnitzii, and a proposal to reclassify it as Faecalibacterium prausnitzii gen. nov., comb. nov. Int J Syst Evol Microbiol 2002; 52:2141-6.

2. Miquel S, Martin R, Rossi O, Bermudez-Humaran LG, Chatel JM, Sokol H, et al. Faecalibacterium prausnitzii and human intestinal health. Curr Opin Microbiol 2013; 16:255-61.

3. Lopez-Siles M, Duncan SH, Garcia-Gil LJ, Martinez-Medina M. Faecalibacterium prausnitzii: from microbiology to diagnostics and prognostics. ISME J 2017; 11:841-52.

4. Martin R, Bermudez-Humaran LG, Langella P. Searching for the Bacterial Effector: The Example of the Multi-Skilled Commensal Bacterium Faecalibacterium prausnitzii. Front Microbiol 2018; 9:346.

5. Sakamoto M, Sakurai N, Tanno H, Iino T, Ohkuma M, Endo A. Genome-based, phenotypic and chemotaxonomic classification of Faecalibacterium strains: proposal of three novel species Faecalibacterium duncaniae sp. nov., Faecalibacterium hattorii sp. nov. and Faecalibacterium gallinarum sp. nov. Int J Syst Evol Microbiol 2022; 72.

6. Sokol H, Pigneur B, Watterlot L, Lakhdari O, Bermudez-Humaran LG, Gratadoux JJ, et al. Faecalibacterium prausnitzii is an anti-inflammatory commensal bacterium identified by gut microbiota analysis of Crohn disease patients. Proc Natl Acad Sci U S A 2008; 105:16731-6.

7. Sokol H, Seksik P, Furet JP, Firmesse O, Nion-Larmurier I, Beaugerie L, et al. Low counts of Faecalibacterium prausnitzii in colitis microbiota. Inflamm Bowel Dis 2009; 15:1183-9.

8. Tilg H, Moschen AR. Microbiota and diabetes: an evolving relationship. Gut 2014; 63:1513-21.

9. Langella P, Guarner F, Martin R. Editorial: Next-Generation Probiotics: From Commensal Bacteria to Novel Drugs and Food Supplements. Front Microbiol 2019; 10:1973.

10. Pryde SE, Duncan SH, Hold GL, Stewart CS, Flint HJ. The microbiology of butyrate formation in the human colon. FEMS Microbiol Lett 2002; 217:133-9.

11. Louis P, Flint HJ. Diversity, metabolism and microbial ecology of butyrate-producing bacteria from the human large intestine. FEMS Microbiol Lett 2009; 294:1-8.

12. Lenoir M, Martin R, Torres-Maravilla E, Chadi S, Gonzalez-Davila P, Sokol H, et al. Butyrate mediates anti-inflammatory effects of Faecalibacterium prausnitzii in intestinal epithelial cells through Dact3. Gut Microbes 2020; 12:1-16.

13. Quevrain E, Maubert MA, Sokol H, Devreese B, Seksik P. The presence of the anti-inflammatory protein MAM, from Faecalibacterium prausnitzii, in the intestinal ecosystem. Gut 2016; 65:882.

14. Quevrain E, Maubert MA, Michon C, Chain F, Marquant R, Tailhades J, et al. Identification of an anti-inflammatory protein from Faecalibacterium prausnitzii, a commensal bacterium deficient in Crohn's disease. Gut 2016; 65:415-25.

15. Auger S, Kropp C, Borras-Nogues E, Chanput W, Andre-Leroux G, Gitton-Quent O, et al. Intraspecific Diversity of Microbial Anti-Inflammatory Molecule (MAM) from Faecalibacterium prausnitzii. Int J Mol Sci 2022; 23.

16. Martin R, Chain F, Miquel S, Lu J, Gratadoux JJ, Sokol H, et al. The commensal bacterium Faecalibacterium prausnitzii is protective in DNBS-induced chronic moderate and severe colitis models. Inflamm Bowel Dis 2014; 20:417-30.

17. Martin R, Miquel S, Chain F, Natividad JM, Jury J, Lu J, et al. Faecalibacterium prausnitzii prevents physiological damages in a chronic low-grade inflammation murine model. BMC Microbiol 2015; 15:67.

18. Duncan SH, Holtrop G, Lobley GE, Calder AG, Stewart CS, Flint HJ. Contribution of acetate to butyrate formation by human faecal bacteria. Br J Nutr 2004; 91:915-23.

19. Charrier C, Duncan GJ, Reid MD, Rucklidge GJ, Henderson D, Young P, et al. A novel class of CoA-transferase involved in short-chain fatty acid metabolism in butyrate-producing human colonic bacteria. Microbiology 2006; 152:179-85.

20. D'Hoe K, Vet S, Faust K, Moens F, Falony G, Gonze D, et al. Integrated culturing, modeling and transcriptomics uncovers complex interactions and emergent behavior in a three-species synthetic gut community. Elife 2018; 7.

21. Lopez-Siles M, Khan TM, Duncan SH, Harmsen HJ, Garcia-Gil LJ, Flint HJ. Cultured representatives of two major phylogroups of human colonic Faecalibacterium prausnitzii can utilize pectin, uronic acids, and host-derived substrates for growth. Appl Environ Microbiol 2012; 78:420-8.

22. Rios-Covian D, Gueimonde M, Duncan SH, Flint HJ, de los Reyes-Gavilan CG. Enhanced butyrate formation by cross-feeding between Faecalibacterium prausnitzii and Bifidobacterium adolescentis. FEMS Microbiol Lett 2015; 362.

23. Wrzosek L, Miquel S, Noordine ML, Bouet S, Joncquel Chevalier-Curt M, Robert V, et al. Bacteroides thetaiotaomicron and Faecalibacterium prausnitzii influence the production of mucus glycans and the development of goblet cells in the colonic epithelium of a gnotobiotic model rodent. BMC Biol 2013; 11:61.

24. Macfarlane S, Macfarlane GT. Regulation of short-chain fatty acid production. Proc Nutr Soc 2003; 62:67-72.

25. Miquel S, Martin R, Bridonneau C, Robert V, Sokol H, Bermudez-Humaran LG, et al. Ecology and metabolism of the beneficial intestinal commensal bacterium Faecalibacterium prausnitzii. Gut Microbes

2014; 5:146-51.

26. Lebas M, Garault P, Carrillo D, Codoner FM, Derrien M. Metabolic Response of Faecalibacterium prausnitzii to Cell-Free Supernatants from Lactic Acid Bacteria. Microorganisms 2020; 8.

27. Kang D, Ham HI, Lee SH, Cho YJ, Kim YR, Yoon CK, et al. Functional dissection of the phosphotransferase system provides insight into the prevalence of Faecalibacterium prausnitzii in the host intestinal environment. Environ Microbiol 2021; 23:4726-40.

28. Harms A, Brodersen DE, Mitarai N, Gerdes K. Toxins, Targets, and Triggers: An Overview of Toxin-Antitoxin Biology. Mol Cell 2018; 70:768-84.

29. Gottesman S. Trouble is coming: Signaling pathways that regulate general stress responses in bacteria. J Biol Chem 2019; 294:11685-700.

30. Saier MH, Jr. A functional-phylogenetic system for the classification of transport proteins. J Cell Biochem 1999; Suppl 32-33:84-94.

31. Sestok AE, Linkous RO, Smith AT. Toward a mechanistic understanding of Feo-mediated ferrous iron uptake. Metallomics 2018; 10:887-98.

32. Lau CK, Krewulak KD, Vogel HJ. Bacterial ferrous iron transport: the Feo system. FEMS Microbiol Rev 2016; 40:273-98.

33. Henry C, Bassignani A, Berland M, Langella O, Sokol H, Juste C. Modern Metaproteomics: A Unique Tool to Characterize the Active Microbiome in Health and Diseases, and Pave the Road towards New Biomarkers-Example of Crohn's Disease and Ulcerative Colitis Flare-Ups. Cells 2022; 11.

34. Hecker M, Schumann W, Volker U. Heat-shock and general stress response in Bacillus subtilis. Mol Microbiol 1996; 19:417-28.

35. Morvan C, Folgosa F, Kint N, Teixeira M, Martin-Verstraete I. Responses of Clostridia to oxygen: from detoxification to adaptive strategies. Environ Microbiol 2021; 23:4112-25.

36. Pi H, Helmann JD. Ferrous iron efflux systems in bacteria. Metallomics 2017; 9:840-51.

37. Heinken A, Khan MT, Paglia G, Rodionov DA, Harmsen HJ, Thiele I. Functional metabolic map of Faecalibacterium prausnitzii, a beneficial human gut microbe. J Bacteriol 2014; 196:3289-302.

38. Pisithkul T, Schroeder JW, Trujillo EA, Yeesin P, Stevenson DM, Chaiamarit T, et al. Metabolic Remodeling during Biofilm Development of Bacillus subtilis. mBio 2019; 10.

39. Berges M, Michel AM, Lassek C, Nuss AM, Beckstette M, Dersch P, et al. Iron Regulation in Clostridioides difficile. Front Microbiol 2018; 9:3183.

40. Chazarreta-Cifre L, Martiarena L, de Mendoza D, Altabe SG. Role of ferredoxin and flavodoxins in Bacillus subtilis fatty acid desaturation. J Bacteriol 2011; 193:4043-8.

41. Bustin SA, Benes V, Garson JA, Hellemans J, Huggett J, Kubista M, et al. The MIQE guidelines: minimum information for publication of quantitative real-time PCR experiments. Clin Chem 2009; 55:611-22.

42. Wattam AR, Abraham D, Dalay O, Disz TL, Driscoll T, Gabbard JL, et al. PATRIC, the bacterial bioinformatics database and analysis resource. Nucleic Acids Res 2014; 42:D581-91.

Additional Files

Additional file 1: Figure S1. Scheme summarizing the experimental set-up and methods used in the study

Additional file 2: Tables S1-S7. RNA-seq data

Additional file 3: Figure S2. Expression of CG447_03795 gene encoding MAM protein across late exponential (E/Ea time points) and early stationary (S/Sa time points) in low (blue symbol) and high (orange symbol) acetate growth condition, using RNA-seq method.

Additional file 4: RNAseq data (read counts) of *feoAB* and *feoAABC* genes in low- and high-acetate conditions: bars of reads counts in late exponential and early stationary phases.

Additional file 5: Tables S1-S6. Metaproteomic data.

Additional file 6: Figure S3 Localisation of the matched peptides (underlined in yellow) of Faecalibacterium FeoB protein sequence and A2-165 feoB protein sequence (underlined in yellow and bold).

Additional file 7: Figure S4. Functional classification workflow in this study

Declarations

Research Ethics and Consent

"Not applicable"

Availability of data and materials

The data that support the findings of this study are openly available in database Omics Dataverse at https://doi.org/10.15454/BDNCT2/ [DOI accession number BDNCT2].

All of the material is owned by the authors and/or no permissions are required.

Competing interests

No, I declare that the authors have no competing interests, or other interests that might be perceived to influence the results and/or discussion reported in this paper.

Funding

This work was supported by the French funding agency “Agence Nationale de la Recherche” under Grant (ANR-16-CE29-0020); under Grant (BP-Acetate, Qualiment- Institut Carnot); and under Grant (ANR-10-INBS-09).

Authors' contributions

E.H., S.L. and M.T. designed research; E.H., S.V., S.C., and Y.J. performed research; E.H., S.V., S.A., S.L., Y.J., C.J., C.H. analysed data; and E.H., S.L., M.T, C.J., S.V., P.L., H.S., C.H., L.B., S.A wrote the paper; and E.H., L.B and M.T, funding acquisition. All read and approved the final manuscript.

Acknowledgements

We acknowledge the sequencing and bioinformatics expertise of the I2BC High-throughput sequencing facility. We thank V. Robert, C. Mayeur, R. Martin and J.M. Chatel for helpful advices, F.Mazouz for RT-PCR analysis and L. Higgins for english correction service.

Figures

Figure 1

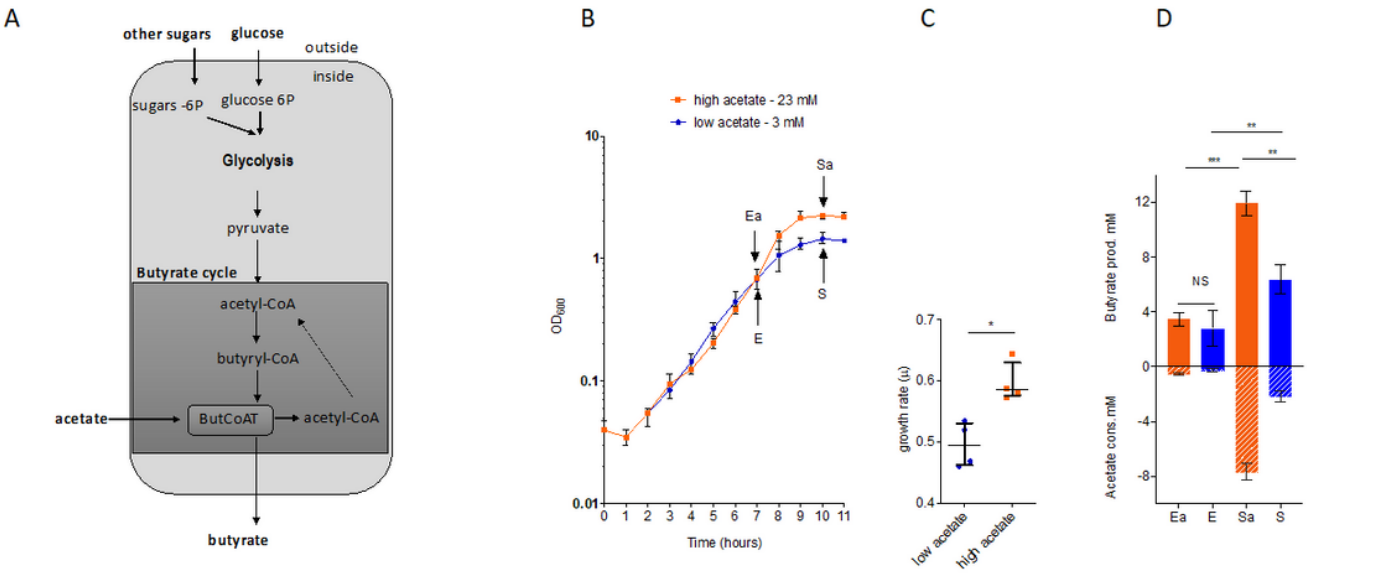

Figure 1

Acetate growth effect and butyrate production in *F. duncaniae* A2-165 cultures. (a) Schematic view of the importance of acetate in the butyrate biosynthetic pathway**.** The production of butyrate is dependent on glycolysis and the butyrate cycle. The key enzyme for butyrate production is butyryl-*CoA*:acetate *CoA*-transferase (ButCoAT), which consumes extracellular acetate to produce butyrate and acetyl-CoA from butyryl-CoA. (b) Growth kinetics of *F. duncaniae* A2-165 under high- and low-acetate conditions. Growth kinetics are shown for bacteria cultured in BHIS medium with 23 mM acetate (high-acetate, orange color) or with 3 mM acetate (low-acetate, blue color). Arrows indicate time points of sampling for the RNA-Seq transcriptome analysis. Sampling was performed after 7 hours (late exponential phase, E and Ea for low- and high-acetate conditions, respectively) and 10 hours (early stationary phase, S and Sa for low- and high-acetate conditions, respectively) of growth. N=4, median with interquartile range (IQR) is shown. (C) Individual growth-rate measures in high/low-acetate conditions. N=4, raw data, median with IQR are shown. (d) SCFA concentrations (expressed as molarity) of E/Ea and S/Sa culture supernatants. Butyrate production is presented as positive values while acetate consumption is presented as negative values. Acetate values were normalized with the acetate value of BHIS medium, which contains 3 mM of acetate. N=4, median with IQR is shown.

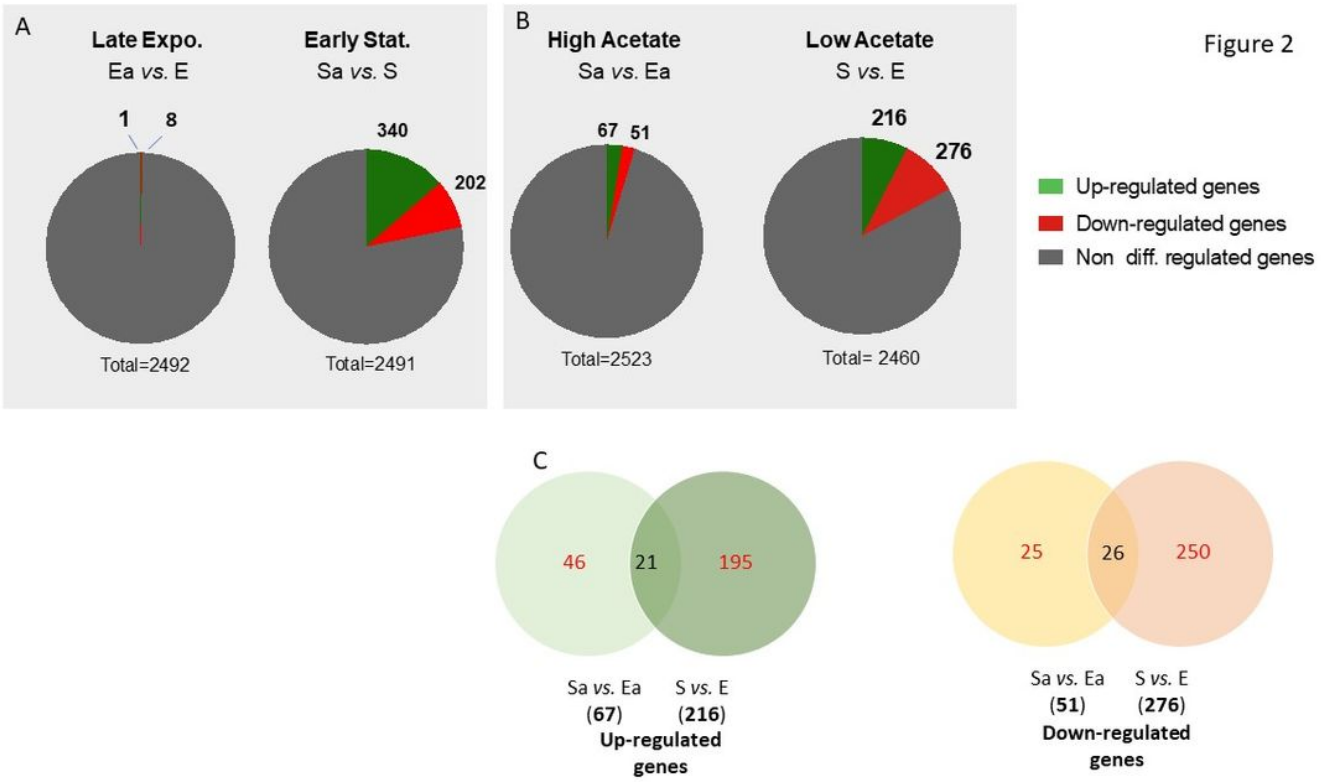

Figure 2

Figure 2

Overview of RNA-Seq data. (a) Two-group comparisons between high- and low-acetate conditions in the late exponential (Ea *vs.* E) and early stationary (Sa *vs.* S) phases. (b) Two-group comparisons between

early stationary and late exponential phases in high-acetate (Sa *vs.* Ea) and low-acetate (S *vs.* E) conditions. Up- and downregulated genes ($\log_2$FC ≥ |2|, FDR-adjusted p-value ≤ 0.01) and non-differentially expressed genes ($\log_2$FC < |2|) are shown. The total number of differentially expressed (DE) and non-DE genes is shown below each pie-chart. (c) Venn diagrams of upregulated and downregulated genes under two conditions. Each diagram was created based on two lists of DE genes. These lists contained 67, and 216 DE genes for the upregulated diagram (left part) and 51, and 276 DE genes for the downregulated diagram (right part). Of the 283 upregulated genes (Sa *vs.* Ea and S *vs.* E lists), 21 genes were held in common, while 46 and 195 genes were specific to the high- and low-acetate conditions, respectively. Of the 327 downregulated genes (Sa *vs.* Ea and S *vs.* E lists), 26 genes were held in common, while 25 and 250 genes were specific to the high- and low-acetate conditions, respectively.

Figure 3A

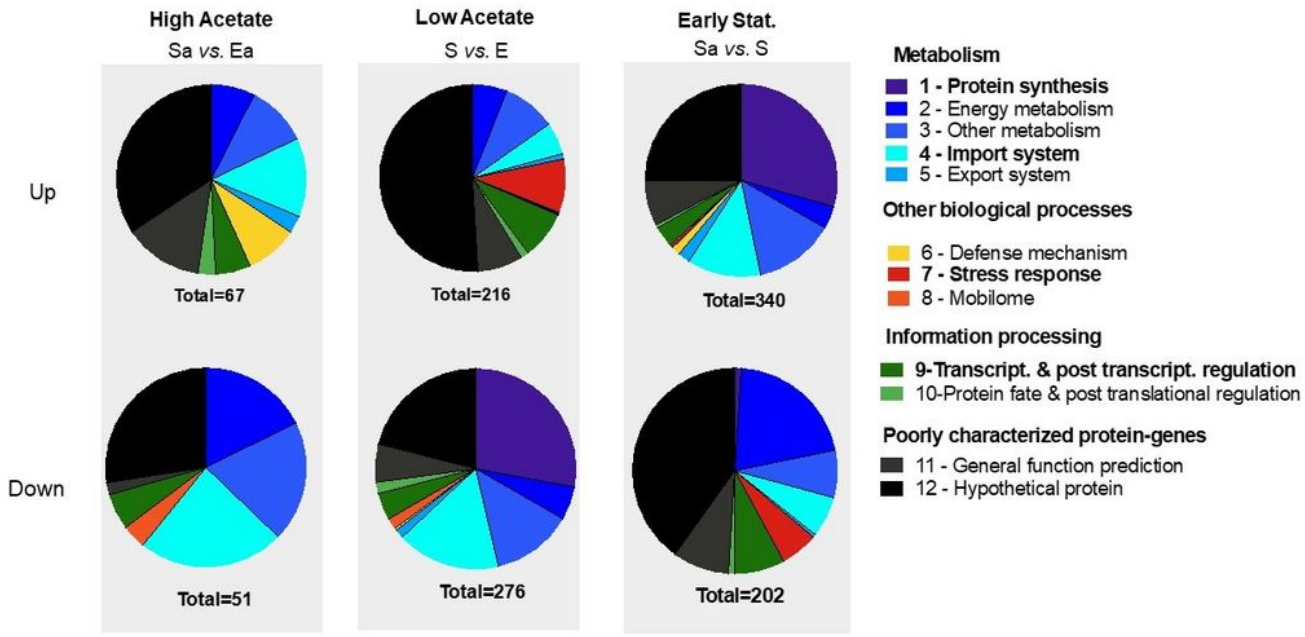

Figure 3B

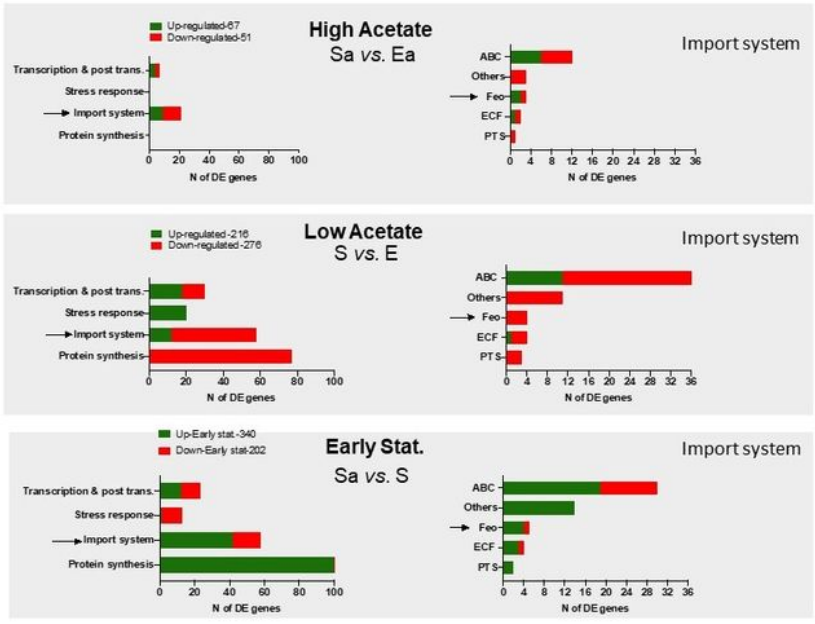

Figure 3

Transcriptional responses of *F. duncaniae* A2-165 to acetate. (a) Pie charts of up- and downregulated genes showing the relative frequency (%) of each functional category. The number of genes in each category is shown in Table S6 in Additional file 2 and the total number of DE genes is shown below each pie-chart. The right part of the panel shows the representative color for each category. The category “Other biological processes” contained the metabolism subcategories “Amino acid”, “Amino sugar”,

"Nucleotide", "Vitamin and Cofactor", "Lipid", and "Cell wall", as well as "Bacterial cell division processes". The "Energy metabolism" category corresponds to the conversion of carbon sources and acetate to ATP and the carbon skeleton and includes glycolysis and the butyrate pathway. See Tables S3–S5 in Additional file 2 for data on DE genes (gene ID, protein annotation, log_2FC, padj value, category). Bold characters indicate category selection in this study. (b) Description of relevant functional categories and import system subclassification in high, low and early stationary acetate transcriptomes. ABC (ATP-binding cassette) transport family. Others: other transport system family, FeoB (Ferrous) iron transport system family. PTS: phosphoenol pyruvate transferase system family, ECF (Energy Coupling Factor) transport family.

Arrows indicate "Import system" category selection and FeoB transport system selection in this study.

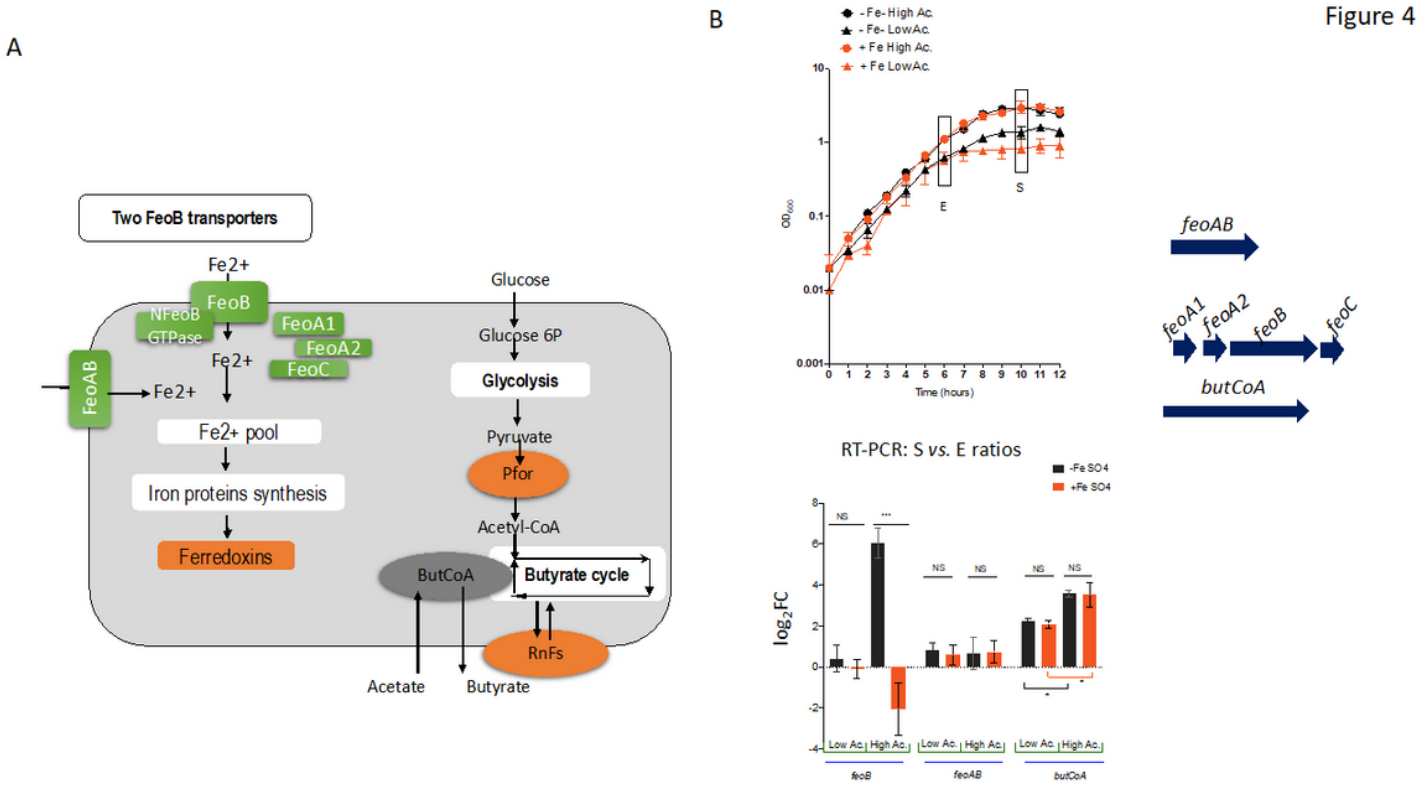

Figure 4

Figure 4

Expression analysis of *feoB*, *feoAB*, and iron uptake system by RT-PCR. (a) Schematic representation of ferrous iron uptake, iron protein synthesis, glycolysis, and butyrate metabolism pathway. The FeoB membrane transporter, NFeoB domain with GTPase activity, and FeoA1, FeoA2, and FeoC cytosolic proteins are indicated. In the FeoB systems that have been described to date, cytosolic proteins are required for ferrous iron acquisition but the exact mechanism is not yet known [31]. The glycolysis pathway and *Faecalibacterium*'s genus-specific butyrate production pathway (shown as butyrate cycle) are shown. Pyruvate is converted to acetyl-CoA by pyruvate:ferredoxin oxidoreductase (PFOR) and the energy generated during butyrate production is conserved through the buildup of a proton gradient via the

activity of a membrane-associated NADH:ferredoxin oxidoreductase encoded by two putative *rnf* operons (*rnfDEA*, CG447_09840-830, *rnfCDGEAB* CG447_10905-930) [37]. Ferredoxin proteins (orange color). See Additional file 2 for data on DE genes (gene ID, protein annotation, log_2FC, padj value, category). (b). Effect of the addition of ferrous sulfate on the transcription of *feoB, feoAB*, and *butCoA* genes, quantified using RT-PCR. Growth kinetics of *F. duncaniae* strain A2-165 in the presence or absence of ferrous sulfate (50 µM) in high-acetate (23 mM acetate) and low-acetate (3 mM) growth conditions. Square: culture sampling at T6 (exponential (E) growth phase) and T10 (early stationary (S) growth phase) time points. Genetic organization of the putative *feoA$_1$A$_2$BC* operon is shown.

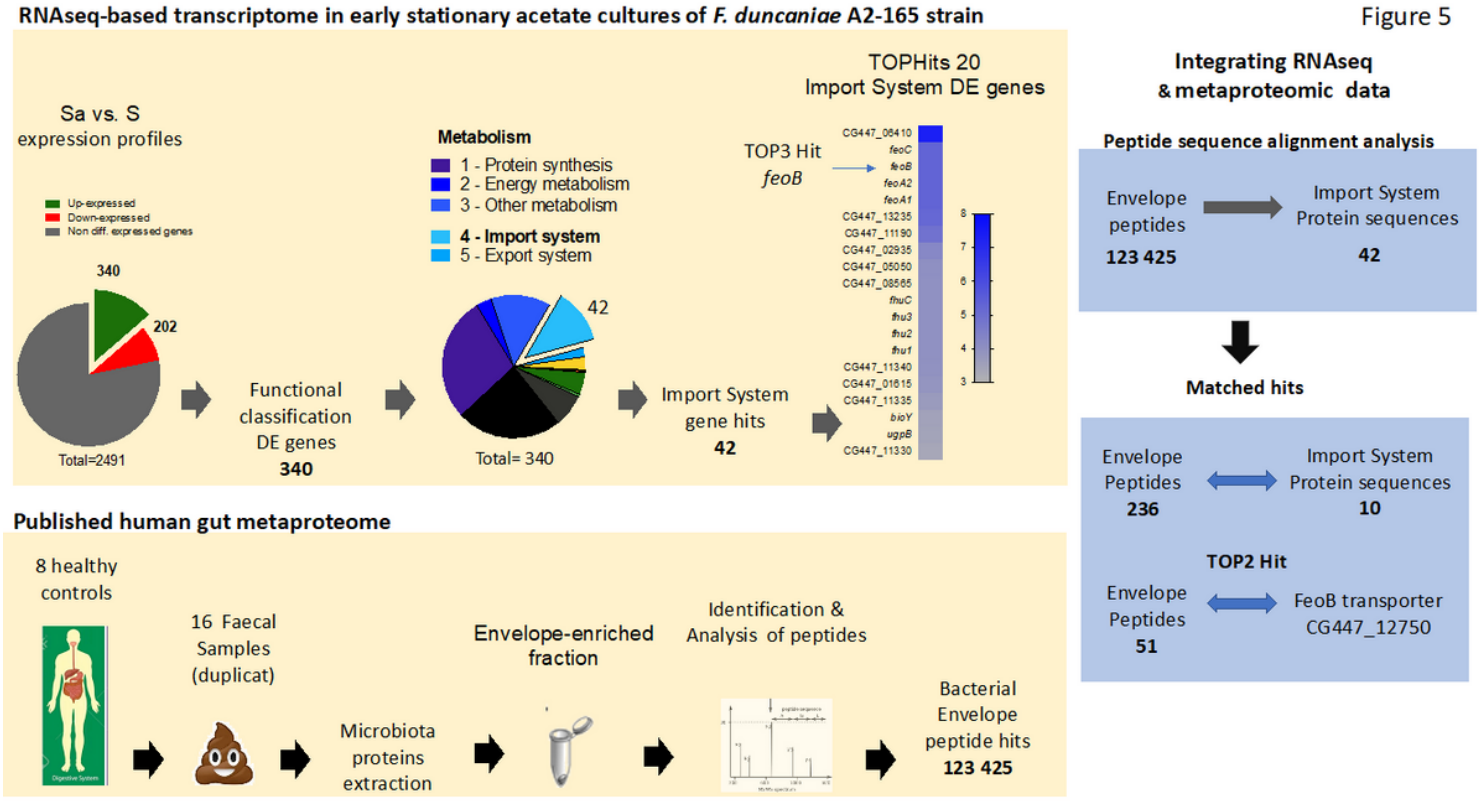

Figure 5

Workflow for the search for FeoB peptides in the healthy human gut metaproteome.

RNA-Seq transcriptome of early stationary acetate cultures of *F. duncaniae* strain A2-165. The general workflow employed for RNA-Seq in the current study: from identification of DE genes in the early stationary phase (Sa vs S comparison) to *feoA$_1$A$_2$BC* operon selection. (b) Published human gut metaproteome. The general workflow employed in a published study of the gut metaproteome. The data were obtained from eight healthy subjects included in a study of intestinal bowel diseases [33]. (C.) Integrating RNA-Seq & metaproteomic data. The general workflow employed to integrate RNA-Seq and metaproteomic data in the current study and the presentation of data for *F. duncaniae* A2-165.

Supplementary Files

This is a list of supplementary files associated with this preprint. Click to download.

- supdataehuillet170223.pptx
- Additionalfile2tablesS1S7170223.xlsx
- Additionalfile4.xlsx